Journal Pre-proofs

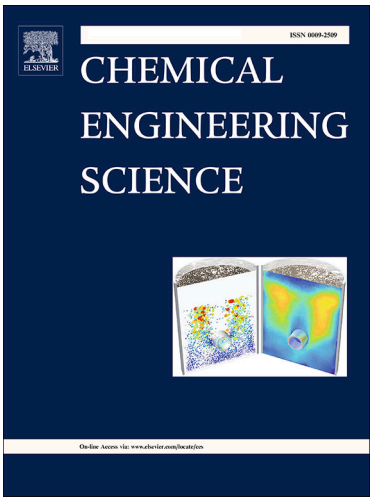

An Experimental Investigation of Dynamic Viscosity of Foam at Different Temperatures

Ahmed Bashir, Amin Sharifi Haddad, Roozbeh Rafati

PII: S0009-2509(21)00827-7
DOI: https://doi.org/10.1016/j.ces.2021.117262
Reference: CES 117262

To appear in: *Chemical Engineering Science*

Received Date: 25 August 2021
Revised Date: 29 October 2021
Accepted Date: 7 November 2021

Please cite this article as: A. Bashir, A. Sharifi Haddad, R. Rafati, An Experimental Investigation of Dynamic Viscosity of Foam at Different Temperatures, *Chemical Engineering Science* (2021), doi: https://doi.org/10.1016/j.ces.2021.117262

An Experimental Investigation of Dynamic Viscosity of Foam at Different Temperatures

Ahmed Bashir, Amin Sharifi Haddad[1], Roozbeh Rafati
School of Engineering, Kings College, University of Aberdeen, AB24 3UE

Abstract

Foam viscosity is a key property to predict the foam flow in narrow channels and porous media. In this study, we investigated the effects of foam quality and temperature on the dynamic foam viscosity and how modifying the composition of colloidal system can alter the foam rheology. It was shown that the addition of nanoparticles and polymer can improve the foam stability at high-temperature conditions and increase the foam apparent viscosity. The results confirmed the foam apparent viscosity can be predicted using a power law model and the flow consistency index of the foam is a strong function of temperature and foam quality, while changes in the power law index with the variation in temperature and foam quality is insignificant.

Finally, to predict the foam apparent viscosity, 3-D plots for the flow consistency and power law indices can be generated as a function of foam quality and temperature.

Keywords:

Apparent viscosity, Foam quality, Power-law model, Shear thinning (pseudo-plastic), Silica nanoparticles, Xanthan gum

1. Introduction

Aqueous foams have been used in narrow channels and porous media for different purposes. This includes their use for displacing hydrocarbons and non-aqueous phases in subsurface porous media. For example, carbon dioxide (CO_2) gas injection, as an Enhanced Oil Recovery (EOR) process, has been widely implemented in many types of reservoirs to improve the

[1] Corresponding author: Amin Sharifi Haddad, Email: amin.sharifi@abdn.ac.uk, Tel: +44 (0)1224 272977 Fax: +44 (0) 1224 272497

reservoir productivity through swelling and viscosity reduction of the oil [1-3]. However, the high gas mobility compared to reservoir hydrocarbons promotes fingering effects and early breakthrough that negatively affect the sweep efficiency of the CO_2 injection process [4,5]. Foam flooding can be an effective strategy to control the CO_2 mobility in a gas flooding process, through improving the CO_2 viscosity, thus lowering its mobility [6-8]. The efficiency of foam flooding is largely controlled by the foam stability and viscosity. Many studies have been conducted to improve the foamability and foam stability by introducing additives such as nanoparticles and polymers and overcome the challenges associated with reservoir conditions [9-13]. The flow properties of the foam are complicated as they depend upon thermodynamic conditions, and hence they are difficult to predict [14,15]. One of these properties is the foam apparent viscosity, which is influenced by foam bubble density, foam quality (the gas fraction), foam morphology, pressure and temperature, chemical additives, salinity, and surfactant concentration among others [9,10,16,17].

Past studies on foam rheological models have shown that foam behaves like a non-Newtonian fluid. Therefore, foam apparent viscosity may increase or decrease with the applied shear rates (or shear stresses) showing shear thickening or shear-thinning characteristics, respectively. In most of the experimental studies, aqueous foams have shown shear thinning behaviour. According to these results, foam rheological behaviour can be explained by using either power-law model [10,16,18-21], Herschel-Bulkley model [22-25], or Bingham Plastic model [26,27]. There are theoretical approaches to find the foam apparent viscosity when it flows through porous media such as population balance models [28,29], and implicit-texture models [30,31], and these models have confirmed a non-Newtonian behaviour for foams should be considered [28].

Ozbayoglu et al. [32], investigated the foam rheology as a drilling fluid in pipes. They used a large-scale experimental set-up where long pipes with 15.24 m length and 0.05 to 0.1 m

diameters at low pressure and ambient temperature conditions. The results demonstrated that for foam qualities between 70% and 80%, the best-fitted model to describe the foam rheology was a power-law model, while for 90% foam quality the Bingham Plastic model was more appropriate. However, their measurements are not applicable for porous media flows as foam bubble sizes in pipes and porous media are not comparable. Moreover, Deshpande and Barigou [33], studied the flow behaviour of foams in vertical pipes and their associated structure and pressure drop as a function of foam flow rate, surfactant type and concentration and foam generator. Their results revealed that, foam rheology was successfully described by a power-law model based on a large amount of experimental data, and an explicit relationship for predicting friction factor in foam flow was generated.

On the other hand, some experimental studies have used Hagen-Poiseuille equation which is applicable to Newtonian fluids, to determine the foam apparent viscosity [34-37]. In this way, apparent foam viscosity needs to be found at any specific shear rate as the foam is a non-Newtonian fluid, and its rheological properties are obtained using Newtonian fluid equations. Cawiezel and Niles [22], experimentally investigated the effect of foam quality, shear rate, temperature and pressure on the foam apparent viscosity using a pipe flow rheometer. The rheological properties of foam were described by the Herschel-Bulkley model, and foam was classified as a pseudo-plastic fluid. Their study demonstrated that, as the foam quality increases (from 50% to 80% quality), foam shows a higher viscosity and an evident pseudo-plastic behaviour. Furthermore, they reported that with rising temperature, the apparent viscosity of the foam drops continuously until it reaches a maximum temperature beyond which no significant viscosity reduction happens. Also, the collected data at low shear rates and high-pressure conditions showed that the foam viscosity increases under such conditions. Li et al. [21] studied rheological properties of foams as fracturing fluid at different temperature, shear rate and foam quality conditions. Their experimental results showed that foam is a shear

thinning fluid and its rheological properties can be described by a power-law model. They also found that the viscosity of the foam fracturing fluid was increased with the higher foam quality and pressure, while it was decreased with increasing temperature and shear rate. Additionally, their power law index, *n*, and consistency index, *K*, strongly influenced by the foam quality and temperature. Since their study was focused on fracturing applications, they did not consider any corrections due to the wall effect on the foam viscosity. Also, they investigated the foam behaviour at foam qualities less than 70%, which means for foam flow in porous media further investigations are needed. This is because of the fact that in foam flow in porous media we are dealing with dry foams, i.e., foam qualities as high as 95%, and foam qualities less than 65% are unfavourable for EOR processes, as foam with less quality corresponds to low apparent viscosity.

Foam with high quality is a drier foam which shows more resistance to flow; thus, it has lower mobility [17]. Osei-Bonsu et al. [38], conducted some experiments to investigate the effect of foam quality on apparent foam viscosity in a 2D Hele-Shaw model and concluded that a dry foam (high foam quality) has higher apparent viscosity. In the other studies that were conducted by Sudhakar and Subhash. [39], and Sani et al. [40], it was found that, in the presence of polymer (xanthan gum, guar gum), high foam qualities produce higher apparent viscosities. In a recent study by Ahmed et al. [15], they investigated the rheological properties of foam at different qualities and textures. Foam apparent viscosity was evaluated by using pressurized foam rheometer at high temperature and pressure conditions (80 ºC and 1500 psi). The foam apparent viscosity increased sharply with the increase of foam quality up to a transition zone and then started to decrease. This decrease in the foam apparent viscosity at very high foam quality condition happens due to the dominance of foam dry-out behaviour in which foam bubbles become drier; thus, the stability of the lamella is reduced due to lamella thinning, which leads to bubbles coalescence.

Many studies have been focused on the effects of chemical compositions on the dynamic properties of foam using capillary viscometer [15,33,38,39]. Results from such studies revealed that, with increasing the surfactant concentration, the foam apparent viscosity was increased. This is attributed to the higher number of free molecules in the interface at high surfactant concentrations, that improves the surfactant elasticity and lowers the surfactant interfacial tension which means the interface has a lower capillary suction from foam films and this improves the apparent viscosity [37,41].

Nanoparticles have shown the ability to generate a stable foam and control the mobility in harsh reservoir conditions for enhanced oil recovery processes [11,12,37,42-46]. The effect of nanoparticles on the mobility control was studied by Farhadi et al. [37], using a capillary viscometer. They used a cationic surfactant and silica nanoparticles (15 nm > 98%) at high pressure and low-temperature conditions. The results revealed that the addition of nanoparticles to the surfactant solution generated relatively small foam bubble sizes, and with increasing the nanoparticles concentration a higher apparent viscosity, compared to the foam with surfactant solution only, was achieved. Therefore, the mixture of nanoparticles and surfactant generated small and uniform bubbles at an optimum nanoparticles' concentration. With increasing the nanoparticles concentration, more particles can participate at the interface, thus increasing the foamability and reducing the foam coalescence and lamella drainage rate. Therefore, higher-pressure drops were observed across the flow test setup, which can be translated to higher apparent viscosities. Yakeen et al. [47] investigated the influence of the different type of nanoparticles on foam apparent viscosity using a Hele-Shaw cell. Foam was generated with CO_2 and sodium dodecyl sulfate (SDS) surfactant at two foam qualities (50% and 75%) in the presence of hydrophilic Al_2O_3, hydrophilic SiO_2 and modified SiO_2 nanoparticles. The results proved that the apparent viscosity increased with increasing the nanoparticles concentration,

hydrophobicity, and foam quality. The increase in the apparent viscosity was due to the adsorption and accumulation of nanoparticles at the foam lamellae and plateau borders.

Polymers as viscosifying agents were introduced to surfactant solutions to improve the foam apparent viscosity (decrease the mobility of displacing fluid) and increase the efficiency of immiscible displacement by foam in porous media. This is because the liquid drainage rate from the lamellae decreases and this reduces the rate of interbubbles gas diffusion [48]. Additionally, Verma et al. [49] reported improvements in foam apparent viscosity by using guar polymer, and increasing the polymer concentration, led to improve the apparent viscosity due to the generation of long structures caused by the interlocking of polymer chains. The enhanced apparent viscosity was due to the conformational changes in the molecular chains induced by electrostatic force and adsorption of surfactant molecules on the polymer chain.

Ahmed et al. [50] studied the effect of using conventional and associative polymers (i.e., superpusher) to improve the foam apparent viscosity under high-pressure and high-temperature conditions (i.e., 10,342 kPa and 80 ºC). The apparent viscosity experiments were conducted using pressurized foam rheometer over a range of shear rates between 10 to 500 s^{-1}. The results revealed that in the absence of polymers, a fast foam decay took place due to the rapid liquid drainage from lamellae. However, in the presence of polymers, foam apparent viscosity was significantly higher due to the slowdown in liquid drainage and the increased foam stability. The associative polymer increased the apparent viscosity much higher than the conventional polymer, which means the associative polymer provides a better mobility control in heterogeneous and fractured reservoirs during the enhanced oil recovery process.

In the past studies, the impact of temperature on the apparent foam viscosity (with different foam qualities) was not investigated extensively. Therefore, the aim of this study is to explore the behaviour of the foam apparent viscosity at different temperatures and foam qualities. This will enable us to develop appropriate rheological models for foam flow in narrow channels and

porous media. Based on the literature, several apparatuses were proposed to investigate the rheological properties of non-Newtonian fluids, such as capillary rheometer, rotating cylinder viscometer, and dynamic stress rheometer [51]. The capillary rheometer is widely used because it is relatively inexpensive and simple to operate [52]; therefore, it was used in this study to characterise the foam rheological properties.

We proposed and tested the use of a power-law model to predict the rheological properties of foam. Additionally, we discussed the effect of temperature on foam apparent viscosity considering different foam qualities, and then we confirmed the same methodology could be used for foams with different chemical compositions.

2. Experimental methodology

2.1. Materials

In this study, Alpha-Olefin Sulfonate (AOS), an anionic surfactant with a viscosity of 1.0 mPa.s at 22 ºC, and a pH of 7.0 - 8.0 was mixed with distilled water. AOS is widely used in EOR processes to provide a low interfacial tension between the displacing and displaced phases while it has shown a low adsorption rate on rock surfaces. The salinity of 2.0 wt% of NaCl was achieved by adding sodium chloride with a purity greater than 99%. Carbon dioxide (CO_2) with a purity greater than 99% was used as our gas phase in all the experiments.

Fumed silica (SiO_2), is a type of nanoparticles, was used in this study. Silica nanoparticles have a molecular weight of 60.08 g/mol and an average particle diameter of 7.0 nm. However, when silica nanoparticles dispersed in the water solution, the Z-average particle diameter was increased to 133 nm [12]. Xanthan gum polymer was used to increase the foam apparent viscosity. Xanthan gum polymer (XG) has a molecular weight of 3.2 million g/mol (molecular weight was measured using a zetasizer nano-zs).

2.2. Setup and procedure

The foam apparent viscosity at high temperature and high salinity was measured using capillary tube rheometer, which was fabricated as a coiled shape tube; the schematic of the setup is shown in Figure 1. The system was designed to measure the dynamic foam viscosity at reservoir conditions. In this study, temperature ranges from ambient up to 80 ºC and a pressure of 345 kPa were considered. The surfactant solution was injected into the system using a high-pressure syringe pump through a piston accumulator, while the CO_2 was injected from a pressurized CO_2 cylinder. The foam was generated in a customized stainless-steel generator (ID= 2.10 cm, L= 6.10 cm), filled with glass beads (size: 500-850 μm) as a porous medium, and they were packed between two stainless steel mesh screens (410 μm) placed in each end of the foam generator. A heating cord was wrapped around the pipes to maintain the system at desired temperature conditions.

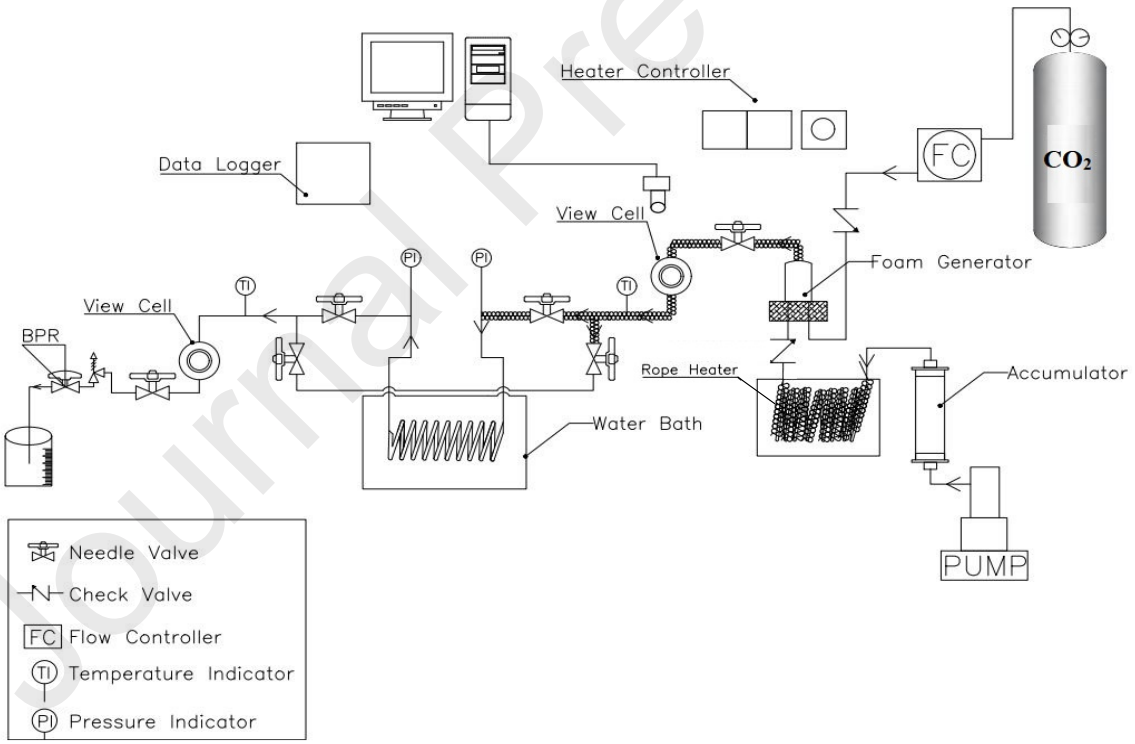

Figure 1. Experimental capillary tube setup for dynamic foam apparent viscosity measurements.

The foam was generated in the foam generator and injected to the stainless-steel capillary tube (ID= 0.136 cm, L= 600 cm) for measuring the apparent viscosity through a pressure difference between the inlet and outlet. The differential pressure along the capillary tube was measured

using two pressure transducers. A water bath equipped with a temperature controller was used to maintain the temperature of the capillary tube at the desired values (25, 50, 80 °C) during the experiment. Foam enters and exits two view cells with 3.3 cm diameter, and 3.2 cm void space thickness that was connected to both ends of the capillary tube to observe the foam characteristics such as foam morphology and the bubble size distribution.

The power-law model was used to calculate the foam apparent viscosity with different composition at various temperature conditions. The foam is treated as a single-phase and incompressible fluid, and at steady-state conditions, the flow in the pipe is resisted by a force at the wall boundary of the system; therefore, the wall shear rate and wall shear stress were calculated as follows [53]:

$$\gamma_w = \frac{32Q}{\pi D^3} = \frac{8\overline{U}}{D} \tag{1}$$

$$\tau_w = \frac{D\Delta P}{4L} \tag{2}$$

where γ_w is the wall shear rate (hereafter we simply call it shear rate), Q is the volumetric flow rate (the total flow rate of gas and liquid), or $\overline{U}$ is the average flow velocity, D is the inner diameter of the capillary tube, τ_w is the wall shear stress, ΔP is the differential pressure between the two capillary ends, L is the length of the capillary tube. However, when computing the foam apparent viscosity as a non-Newtonian fluid from the collected data (using the capillary rheometer), the shear rate (γ_w) in Equation (1) must be corrected by applying the Weissenberg-Rabinowitsch correction model [56]. Equation (1) is only valid for Newtonian fluids, and non-Newtonian fluids with shear thinning behaviour, experience significantly higher shear rate at the wall compared to Newtonian fluids [54]. Therefore, the true shear rate (corrected shear rate) (γ_T) at the wall for the non-Newtonian fluid was calculated by using:

$$\gamma_T = \gamma_w\left(\frac{3}{4} + \frac{1}{4}\frac{d\ log\left(\frac{8\overline{U}}{D}\right)}{d\ log\ (\tau_w)}\right) \tag{3}$$

Let us define

$$n' = \frac{d\,log\,(\tau_w)}{d\,log\left(\frac{8\overline{U}}{D}\right)} = \frac{d\,log\,(\tau_w)}{d\,log\,(\gamma_w)} \quad (4)$$

Therefore,

$$\gamma_T = \gamma_w\left(\frac{3n'+1}{4n'}\right) \quad (5)$$

Where n' is the slope of the log-log plot of the flow curve. Based on Equation (4) the flow curve equation is defined as,

$$\tau_w = K' {\gamma_w}^{n'} \quad (6)$$

Since capillary end effects are negligible for long capillary tubes, therefore, the power-law index, n', can be simply shown by n, and the consistency index, K can be calculated as,

$$K = K'\left(\frac{4n}{1+3n}\right)^n \quad (7)$$

Where K' has the same value as the wall shear stress, τ_w, at γ_w= 1 s^{-1}. The apparent viscosity of the foam at any shear rate is given as,

$$\mu_{app} = K(\gamma_T)^{n-1} \quad (8)$$

The foam quality is defined as the percentage of gas volume to the total volume of the foam and calculated using the gas and liquid flow rates:

$$f_q = \frac{Q_g}{Q_g + Q_l} \quad (9)$$

where f_q is the foam quality, Q_g is the gas flow rate, and Q_l is the liquid flow rate. Six different foam qualities from 55%to 97% (foam quality achieved by changing gas and liquid flow rates) were used at different shear rates ranging between 280 and 1200 s^{-1} corresponding to the volumetric flow rates between 4.2 and 16.8 mL/min.

2.3. System calibration

The experimental setup was calibrated using both Newtonian (distilled water) and non-Newtonian (xanthan gum polymer solution) fluids, to ensure it is accurate and precise for rheology tests. The viscosities of water (20 °C) and xanthan gum solution (25 °C) with a concentration of 0.3 wt%, were measured at different shear rates, and they were compared with

the viscosity of water reported in the literature and the viscosity readings from the Rheometer DHR-3 for xanthan gum polymer solution.

Water is a Newtonian fluid with a constant viscosity of 1.002 mPa.s at 20 °C [55]. Figure 2a confirms the outcome of the capillary tube is reasonable as the slope of the shear stress versus shear rate gives 1 mPa.s for the viscosity of water (a straight line with a slope 1.0). Moreover, Figure 2b shows that at different shear rates, the water viscosity is almost constant (1.0 mPa.s) based on the estimated viscosity from the capillary tube that is comparable to the data from the literature. We believe the minor fluctuations in calculated viscosity values in Figure 2b (slightly higher values compared to the reference numbers at shear rates higher than 2000 s^{-1}), can be attributed to the possible turbulent flow effect at higher shear rates.

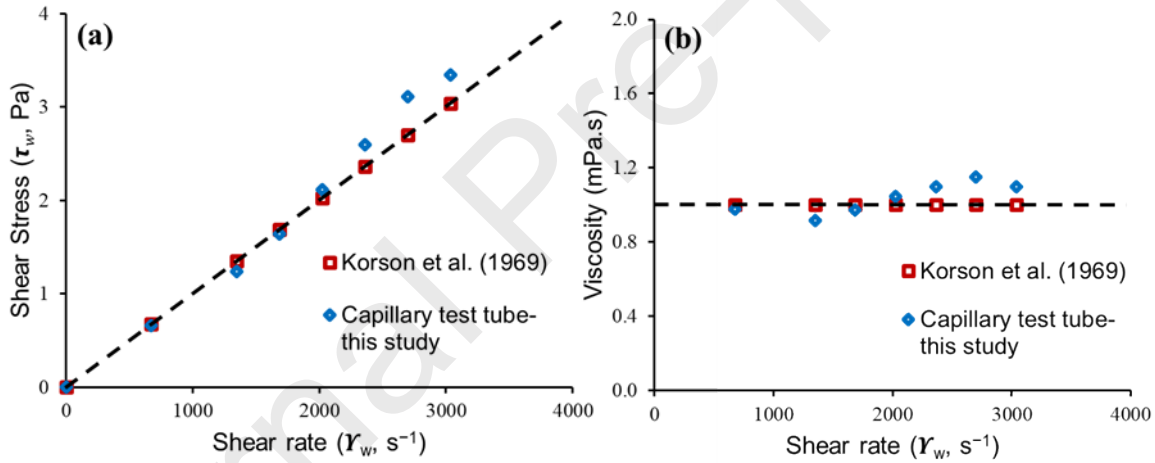

Figure 2. (a) shear stress versus shear rate, and (b) viscosity versus shear rate, for distilled water at 20 °C.

Xanthan gum polymer solution is a non-Newtonian fluid, and as shown in Figure 3 (a & b), the solution demonstrated a pseudo-plastic behaviour; the viscosity was decreased with increasing the shear rates. Furthermore, we compared the viscosity values of the capillary tube test with the outputs from the Rheometer DHR-3. Based on the observations from Figure 3, we could conclude that the data collected from the capillary tube test are within +/-10% (error bars were calculated as the standard deviation obtained from three independent measurements) of data from other experimental apparatus.

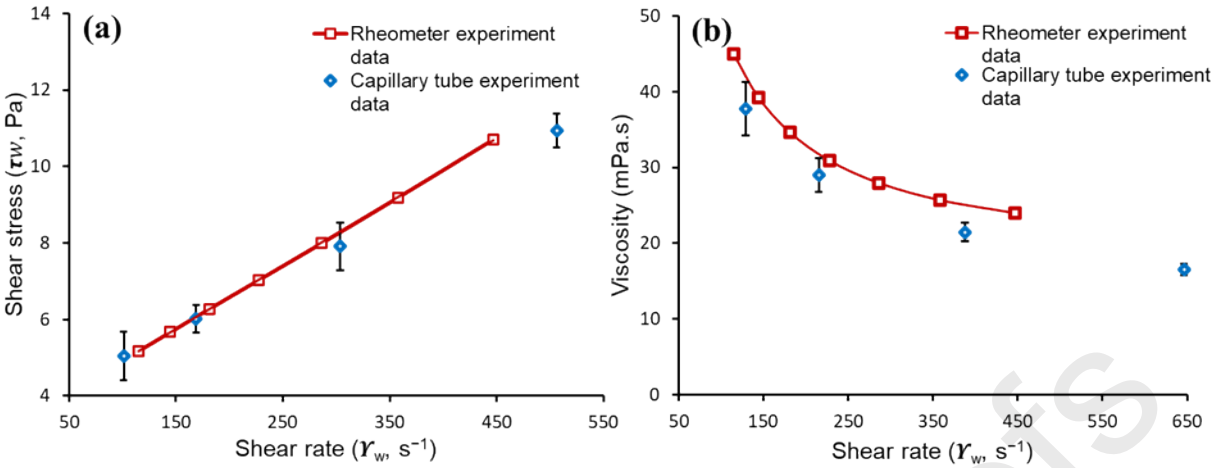

Figure 3. (a) shear stress versus shear rate, and (b) apparent viscosity versus share rate, for xanthan gum polymer solution at 25 °C.

3. Results and discussion

3.1. Effect of shear rate on apparent viscosity

The wall shear rate and wall shear stress for foam (surfactant concentration of 0.5 wt%) with foam qualities between 55% and 97% at 25 °C were plotted in Figure 4. By applying the power-law model for shear rate versus shear stress, we calculated the characteristic parameters (n & K) for each foam quality. The power-law index, n, for each foam quality is the slope of the log-log plot of shear stress versus shear rate, and the consistency index (K) is determined using Equation 7. The n and K values for different foam qualities are listed in Table 1. For all foam qualities, $n < 1$ implied a shear-thinning behaviour.

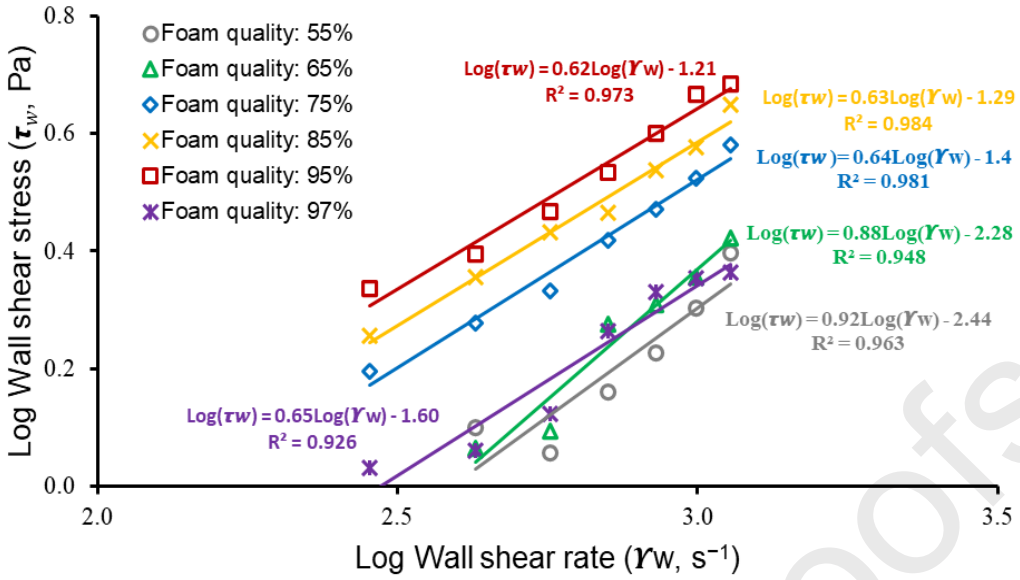

Figure 4. Wall shear rate and wall shear stress for the foam at different foam quality at 25 °C.

Table 1. *n* and *K* values for different foam qualities at 25 °C

Foam quality	*n*	*K* (Pa.s^n)
55%	0.92	0.35×10^{-2}
65%	0.88	0.5×10^{-2}
75%	0.64	3.7×10^{-2}
85%	0.63	4.6×10^{-2}
95%	0.62	5.7×10^{-2}
97%	0.65	2.3×10^{-2}

3.2. Effect of foam quality on apparent viscosity

The foam apparent viscosity was determined from the true shear rate (corrected shear rate at the wall of the capillary tube) using the power-law model accordingly. Therefore, the effect of applied true shear rate on the apparent viscosity of the foam at different foam qualities is presented in Figure 5. The changes in apparent viscosity at different shear rates demonstrate a shear-thinning behaviour under a shear rate ranging from 280-1200 s^{-1}, i.e., the apparent viscosity is decreasing with increasing the shear rate at all foam qualities. Moreover, Figure 5a shows that, foam at qualities between 55 to 65% (wet foam regime) behaves almost like a Newtonian fluid (foam viscosity slightly changed with the shear rates). While for foam quality higher than 65% (dry foam regime), the foam viscosity largely increased with increasing the

foam quality, which is demonstrating a strong shear thinning behaviour. Therefore, the drier the foam the higher the apparent viscosity (in the presence of stable foam with no bubbles coalesce or rupture).

Based on the past studies on the rheological properties of foam [36,38,65-59], as the foam quality increases from 60%, its apparent viscosity increases gradually up to the foam quality of around 80%, and then it becomes noticeable at qualities above 80%. The maximum viscosity would occur at a foam quality near 95%, followed by a marked drop in viscosity at qualities above 95%. This is due to the fact that foams above 95% quality have such a small amount of foaming agent, thus their thin lamellae promote the bubble coalescence [36,59]. Figure 5b demonstrates the effect of increasing foam quality on the foam apparent viscosity at both low shear rate (284 s^{-1}) and high shear rate (1136 s^{-1}). Foam apparent viscosity slightly increased when the quality increased from 55% to 65%, followed by a sharp increase to the peak value when the foam quality reached 95%, and then dramatically decreased as foam quality increased to 97% for both shear rates. This drop in foam apparent viscosity is due to the foam limiting capillary pressure where the foam dry-out behaviour dominates, and bubbles start to coalesce and make a continuous gas phase.

Figure 5 supports the notion that dry foams (capillary pressures less than the limiting capillary pressure value) with higher gas fraction (high quality) require more deformation to yield and flow hence have higher yield stress and subsequently expected to have lower mobility [38,60]. In contrast when wet foams (low quality) are produced, foams are more mobile than dry foams because in wet foams bubbles are more loosely packed due to the presence of high liquid fraction; thus, foam will move easily; which corresponds to low foam apparent viscosity. While

dry foams bubbles are closely packed which result in high resistance to flow; thus, foam apparent viscosity increased.

It should be noted that changes in the foam rheology with foam qualities, depend on the foam chemical composition. For the AOS derived foam compositions in this study, the foam apparent viscosity reached its maximum at the foam quality of 95%, and it is expected at a foam quality higher than 95%, the foam coalescence starts to happen. Since foam qualities more than 95% are practically unimportant, we decided to limit our foam tests up to a maximum foam quality of 95% in the next sections.

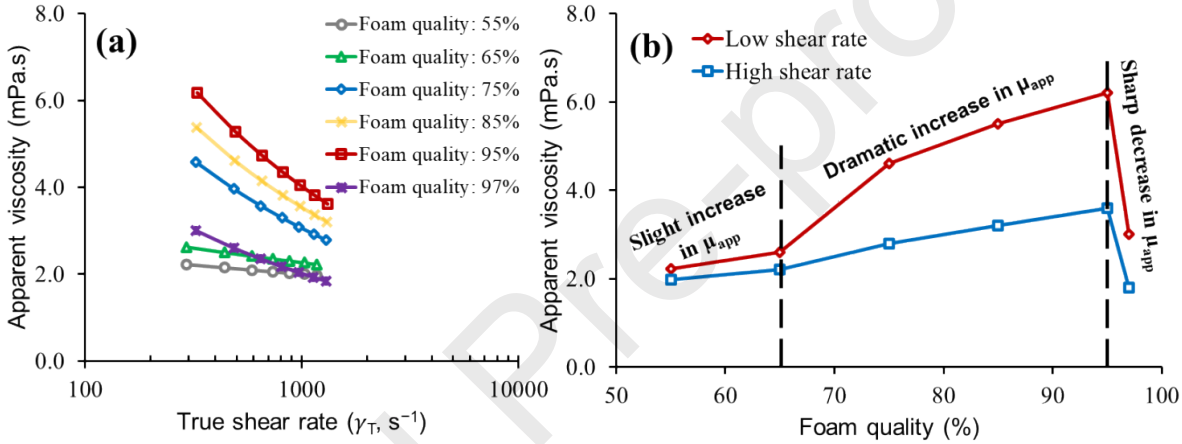

Figure 5. Foam apparent viscosity, as a function of (a) true shear rate, and (b) foam quality at 25 °C.

In addition to the foam quality that has an important effect on the rheological properties of foam, temperature influences these properties; therefore, the foam apparent viscosity at different temperatures and foam qualities should be investigated. This leads to a better understanding of the foam behaviour and developing models that can capture critical variables involved in the rheological properties of foam.

3.3. Effect of temperature on apparent viscosity

Temperature has a significant effect on the foam apparent viscosity in two ways, firstly the viscosity of liquid phase in lamellae decreases with increasing the temperature which means faster liquid drainage rate from lamellae will occur [8,52]; secondly, high temperature can decompose the surfactant present in the foam reducing the surfactant concentration in the

bubble lamellae. This reduced surfactant concentration eventually causes the bubble to destabilize since there is not enough surfactant to be distributed over the liquid film between bubbles (Marangoni effect) [10,22,61]. Therefore, increasing temperature can expedites the liquid drainage in the lamellae and foam dry-out process, and hence reduce the foam apparent viscosity. We investigated the foam apparent viscosity at different temperature conditions (25, 50 and 80 °C). As shown in Figure 6, by increasing the temperature, the apparent viscosity decreases for the three foam qualities. This is attributed to the decrease in the liquid viscosity in the lamellae at the high-temperature condition, which in turn causes faster liquid drainage from the foam structure and eventually foam coalescence, hence decreasing foam viscosity.

Friedmann et al. [62] experimentally showed that foams with higher qualities (e.g., 90%) were more stable and propagated better than foams with low qualities (e.g., 40%) in porous media. Therefore, this is important, for example in foam EOR processes, to achieve a higher apparent viscosity and better mobility control; thus, higher foam qualities between 75% and 95% are investigated in more details for the rest of this study.

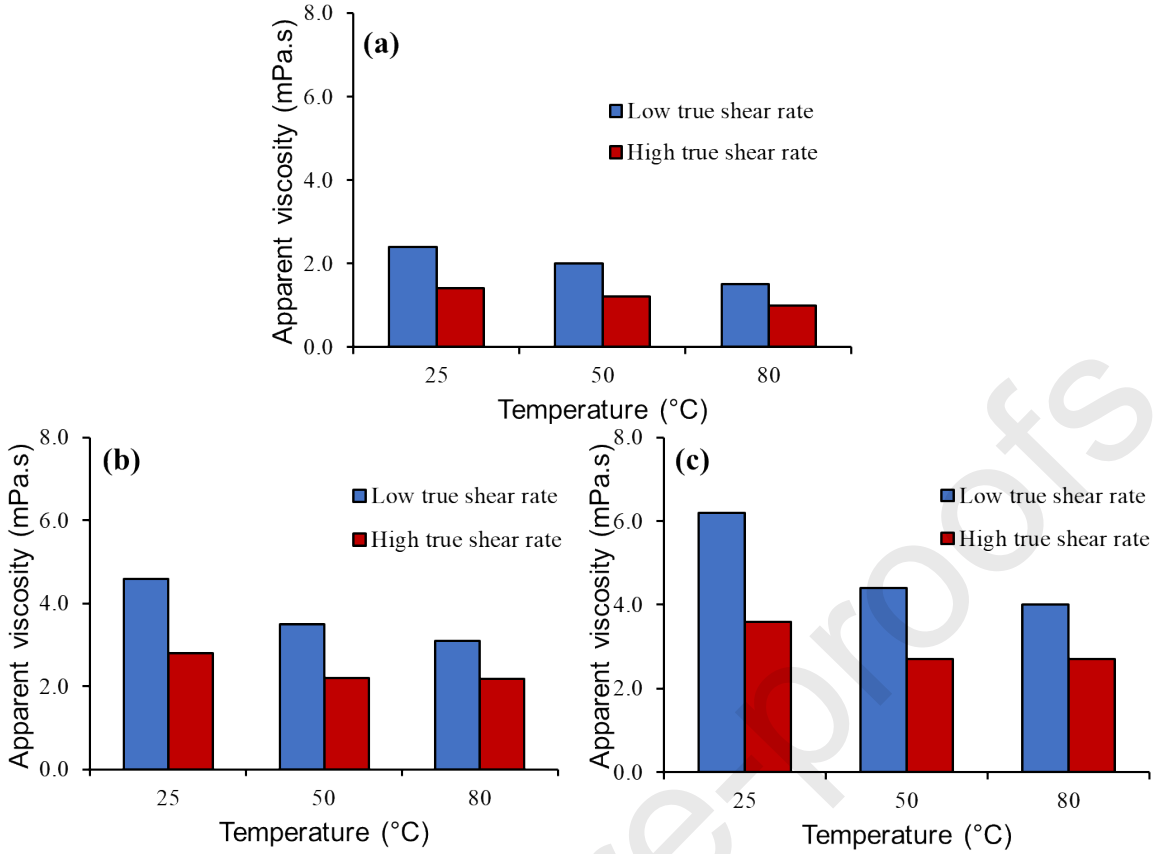

Figure 6. Foam apparent viscosity at different temperature conditions at low (310 to 340 s^{-1}) and high shear rates (1220 to 1370 s^{-1}), with foam quality of (a) 65%, (b) 75% and (c) 95%.

Figures 7 and 8 show that when the temperature increased from 25 to 80 °C, the foam apparent viscosity decreased for both 75% and 95% foam qualities. The inset images in Figures 7 and 8 were taken at the same wall shear rate of 284 s^{-1} (true share rates reported in the inset images correspond to this wall shear rates, after applying the Weissenberg-Rabinowitsch correction model) show the foam morphology changed from small bubbles to coarse bubbles as the temperature increased. This is consistent with the outcomes of previous studies that have confirmed that the foam stability decreases at higher temperatures due to the increase in the drainage rate from the thin lamellae, which caused a higher bubble coalescence rate [12].

Moreover, the reduction in the apparent viscosity, when the temperature increased from 50 to 80 °C, is smaller compared to the reduction when the temperature increased from 25 to 50 °C. This can be speculated when the temperature increases from 25 to 50 °C, most of the liquid in the lamellae quickly starts to drain, leaving behind the thin lamellae; thus, the bubbles stability

and apparent viscosity decrease significantly. A small volume of liquid is remained in the lamellae after the temperature has reached 50 °C. Therefore, any further increase in the temperature will cause a small reduction in the apparent viscosity, and the rate of the coalescence of the bubbles decreases.

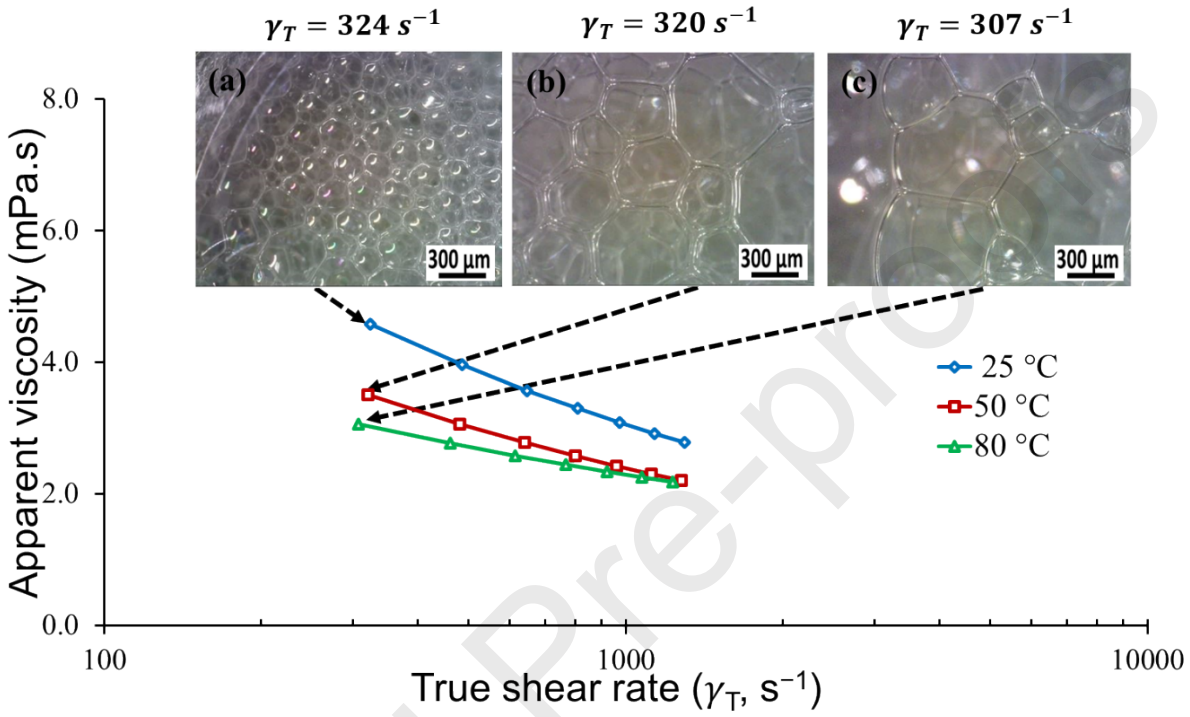

Figure 7. Foam apparent viscosity with 75% foam quality at different temperature conditions, foam morphologies are shown by inset images taken at the same flowrate at (a) 25°C, (b) 50°C, and (c) 80°C.

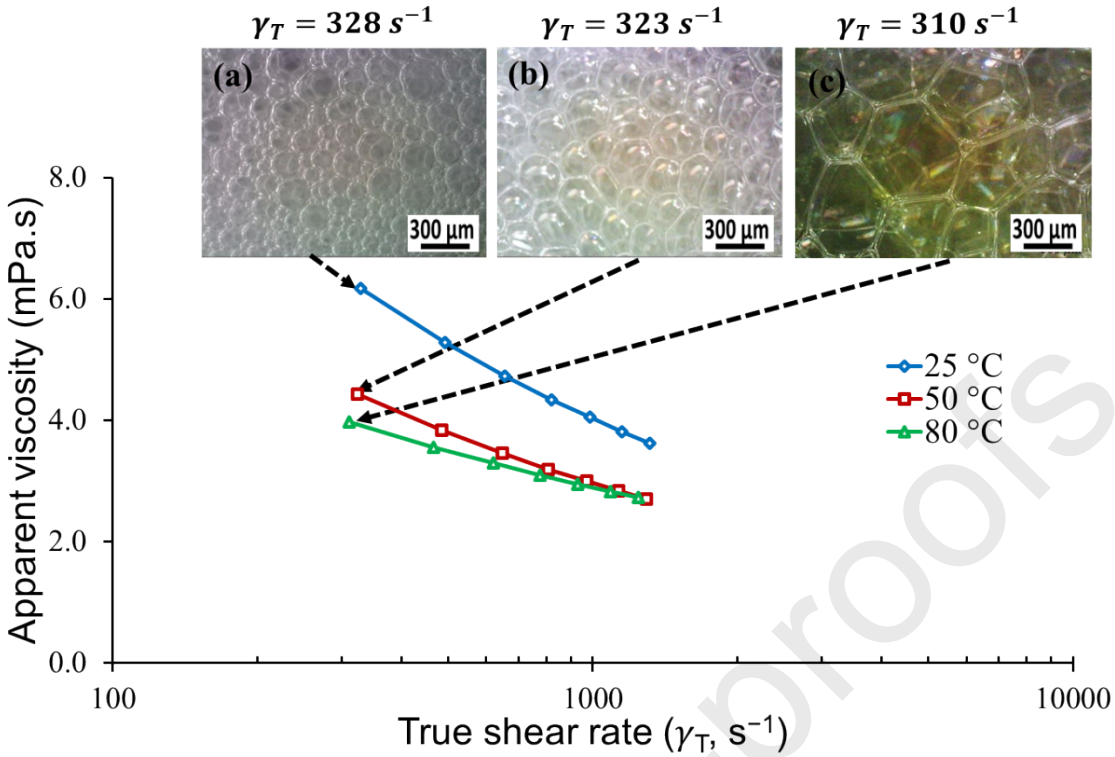

Figure 8. Foam apparent viscosity with 95% foam quality at different temperature conditions, foam morphologies are shown by inset images taken at the same flow rate (a) 25°C, (b) 50°C, and (c) 80°C.

3.4. Effect of composition on apparent viscosity

Foam apparent viscosity were measured for foams with different chemical compositions. Additives such as salt (sodium chloride (NaCl) in this study), nanoparticles (SiO_2), and polymer (xanthan gum) were added to produce three additional foam compositions that are derived from AOS. We then evaluated the effect of composition on the foam apparent viscosity at different temperatures and foam qualities. The results showed that salinity had a negative effect on the foam apparent viscosity. On the other hand, the presence of nanoparticles and polymer compensated the detrimental effect of high temperature and salinity in two foam qualities of 75% and 95% that were tested in this study. More details about the effect of each parameter on the foam apparent viscosity will presented below.

3.4.1. NaCl in the foam composition

In the presence of sodium chloride salt (NaCl), the apparent viscosity was significantly decreased compared to the apparent viscosity in the absence of NaCl for both foam qualities,

as shown in Figure 9 and 10. As it is shown in these figures, the salinity has a detrimental effect on the foam apparent viscosity, at a low shear rate, the apparent viscosity sharply decreased from 5.0 to 2.3 mPa.s and from 6.2 to 3.1 mPa.s for 75% and 95% foam qualities, respectively. This is because the presence of NaCl compresses the double adsorption layer of the surfactant at the gas-liquid interface, which results drainage of the surfactant from the lamellae. This causes a decrease in disjoining pressure between bubbles which in turn increases the bubble sizes and reduces the foam viscosity [63]. These have been demonstrated by the inset images in Figures 9 and 10 (images correspond to the same flowrate or same wall shear rate of 284 s^{-1}) where salinity affected the bubbles texture, sizes, and shapes. For both foam qualities, in the absence of NaCl, the generated foams have uniform bubbles with small sizes, which improved the foam stability and in turn provided high resistance to flow or high viscosity. While, in the presence of NaCl, the generated foams have less uniform with bigger sizes bubbles; consequently, these foams have lower stability, and their viscosities were lower.

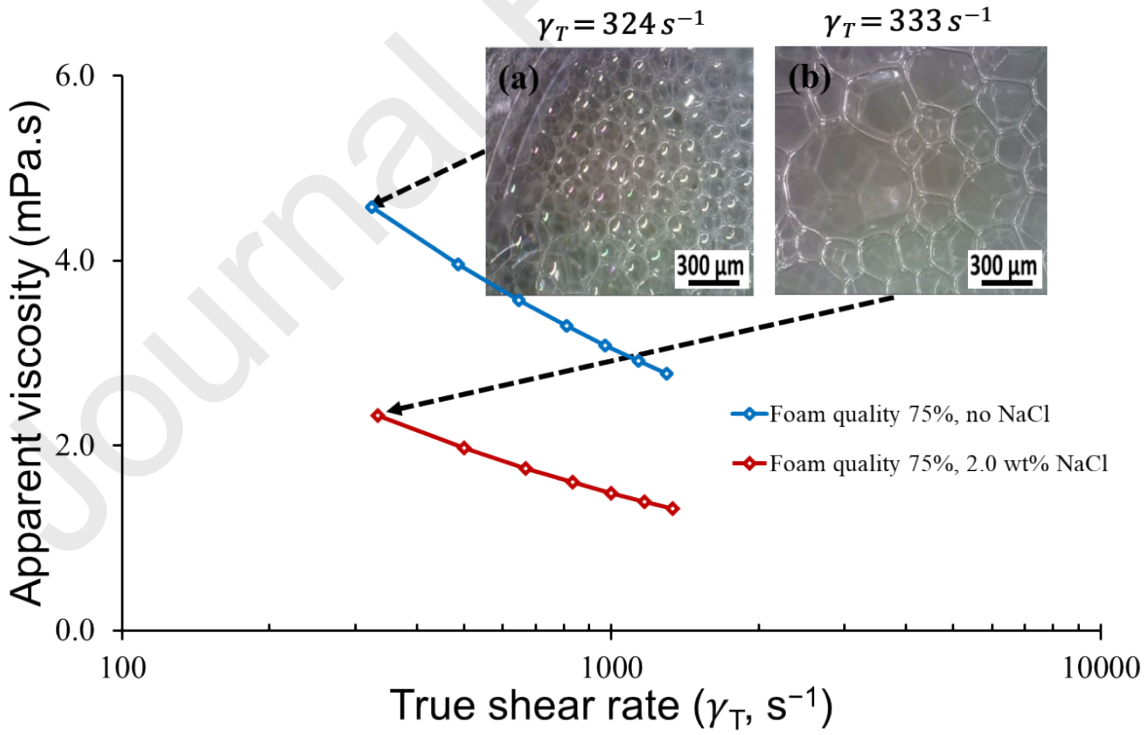

Figure 9. Foam apparent viscosity with 75% foam quality at 25 °C, foam morphologies are shown by inset images taken at the same flow rate (a) in the absence of NaCl, and (b) in the presence of NaCl.

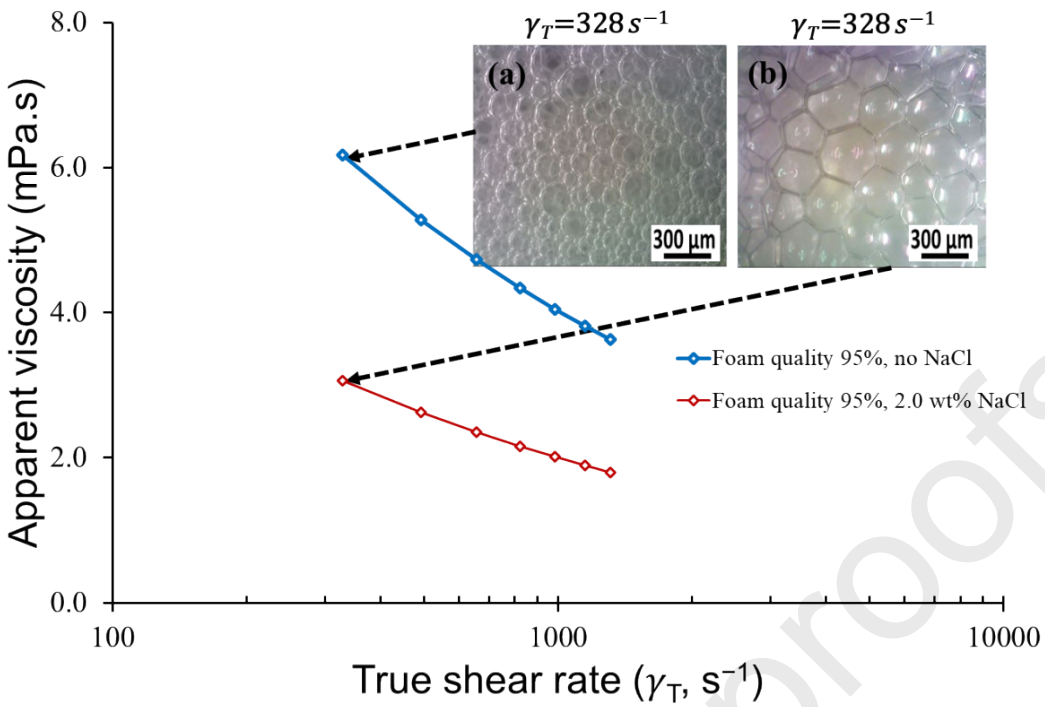

Figure 10. Foam apparent viscosity with 95% foam quality at 25 °C, foam morphologies are shown by inset images taken at the same flow rate (a) in the absence of NaCl, and (b) in the presence of NaCl.

3.4.2. NaCl, nanoparticles & polymer in the foam composition

Nanoparticles and polymer are used to improve the foam apparent viscosity through enhancing the foam stability under elevated temperature conditions. It is hypothesized that, in the absence of nanoparticles and polymer, foam stability dominated by a weak electrostatic repulsion force between the head group of the surfactants adsorbed at the air-water interface. As shown schematically in Figure 11a, this results in a thin lamellae layer due to the fast liquid drainage. Additionally, the presence of salt (NaCl) reduces the availability and the adsorption of surfactant molecules at gas-liquid interfaces of the foam as shown in Figure 11b. Moreover, the reduction in disjoining pressure and closer packing of the thin liquid films between bubbles, due to shielding effect of electrostatic double layer in the presence of salt, lead to bubble coalescence by increase the frequency of bubble collision and coarsening. It should be noted that since one of the factors that improve the foam apparent viscosity is flow resistance of the liquid between the bubbles; reducing this resistance as a result of faster liquid drainage rate from lamellae, leads to lower foam stability and apparent viscosity. In foam systems with

nanoparticles (SiO_2 NPs), NPs disperse at the gas-liquid interface, as shown in Figure 11c. It is expected that, this creates electrical double layers that cause further repulsions between NPs and making the foam lamellae thicker, also this can help to overcome the capillary pressure and prevents gas diffusion from neighbouring bubbles [12,64]. Moreover, the presence of the NPs at the gas-liquid interfaces results in a reduction in their surface tension [65,66]. This probably leads to an improved foam stability and reduces the drainage rate of the surfactant from the lamellae film; as a result, small and spherical bubbles with thicker liquid film will exist, and hence the foam apparent viscosity can be improved. Besides the effects of SiO_2 NPs on improving the foam apparent viscosity, the presence of XG enhances the viscosity of surfactant solution and forms a dense layer (surfactant molecular binds to the polymer chain) with thicker lamellae as shown in Figure 11d. Similarly, these mechanisms decrease the rate of liquid drainage from the lamellae and increases the flow resistance between bubbles (polymer forms bridge between bubbles); thus, an increase in the foam apparent viscosity was observed.

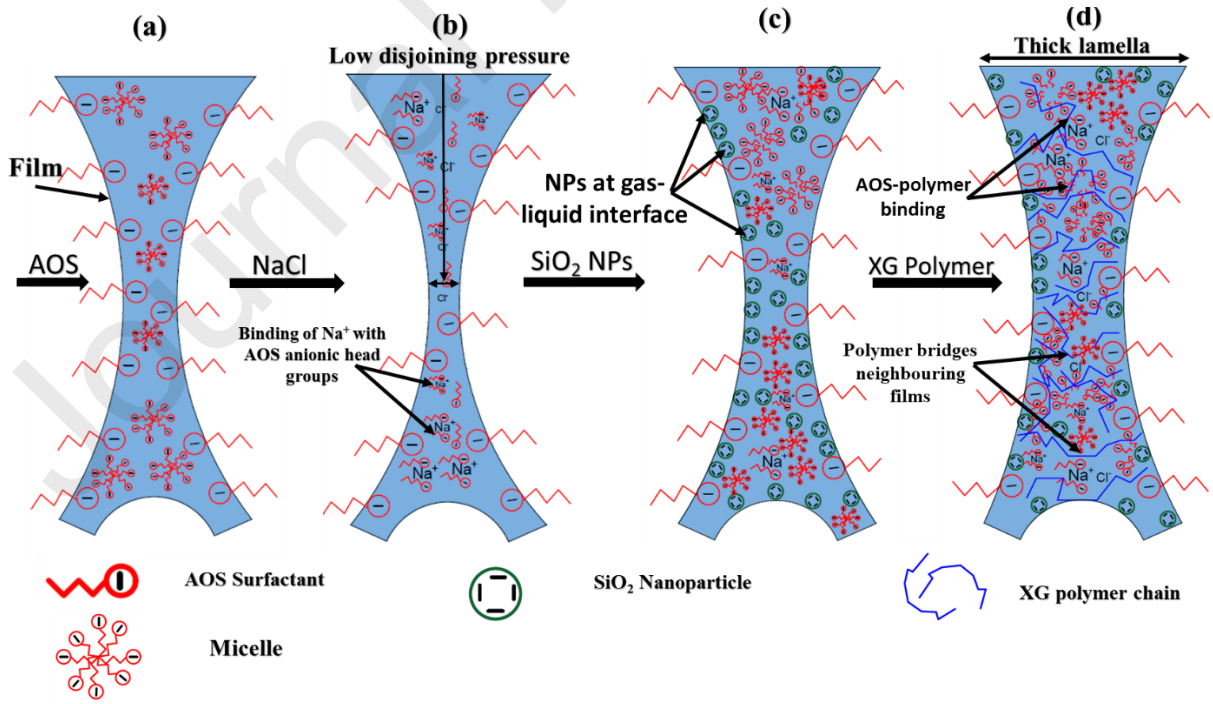

Figure 11. A schematic of the foam lamella stability in the presence (a) AOS surfactant, (b) AOS and NaCl, (c) AOS surfactant, NaCl and SiO_2 NPs, and (d) AOS surfactant, NaCl, SiO_2 NPs and XG polymer.

The optimum concentrations of nanoparticles and polymer that were reported by the previous investigators are used in this study to investigate the effect of temperature and foam quality on the foam apparent viscosity [11,12]. Hence, silica nanoparticles (SiO_2 NPs) and xanthan gum polymer (XG) with 0.2 wt% and 0.3 wt% concentrations, respectively, were added to a surfactant solution with 0.5 wt% AOS and 2.0 wt% NaCl. The relationships obtained between the foam apparent viscosity and the shear rate in the presence of different additives at different temperatures and foam qualities are presented in Figure 12. It can be observed that the foam apparent viscosity has significantly improved in the presence of SiO_2 NPs for both foam qualities of 75% and 95% at all temperatures. As shown in Figure 12 (d and e) the foam apparent viscosity for the foam quality of 95% at lower shear rates were increased by 1.4 to 1.6 times; from 3.1 mPa.s to 4.3 mPa.s at 25 °C, from 2.8 to 3.8 mPa.s at 50 °C, and from 1.9 to 3.1 mPa.s at 80 °C. At the higher shear rates, it was increased by 1.2 to 1.4 times; from 1.8 to 2.2 mPa.s at 25 °C, 1.7 to 2.2 mPa.s at 50 °C, and from 1.4 to 1.9 mPa.s at 80 °C. Similar qualitative behaviour for the improvement of foam apparent viscosity was observed for the foam quality of 75%, as shown in Figure 12 (a and b). These changes are attributed to the adsorption of SiO_2 NPs on the gas-liquid interface, which increases the liquid film thickness by creating repulsive forces through the NPs surface charges and helps to protect the foam bubbles from the rupture and coalescence. Moreover, this reduces the liquid drainage from the lamellae; and increases the pressure drop across the capillary tube. Therefore, the presence of SiO_2 NPs increases the foam apparent viscosity of foam at different temperature conditions, with more improvement at 95% quality.

The addition of XG polymer to SiO_2 NPs can further improve the foam apparent viscosity for both foam qualities of 75% and 95%, at different temperature conditions. Figure 12 (d, e, and f) show that the foam apparent viscosity for the foam quality of 95% at lower shear rates (310 to 340 s^{-1}) increased by 1.3 to 1.5 times; from 4.3 to 6.3 mPa.s at 25 °C and from 3.8 to 4.9

mPa.s at 50 °C and from 3.1 to 4.2 mPa.s at 80 °C when the polymer was added to the foaming agent that had SiO_2 NPs. At higher shear rates (1220 to 1370 s^{-1}), the foam apparent viscosity increased by 1.3 to 1.6 times; from 2.2 to 3.5 mPa.s at 25 °C and from 2.2 to 2.8 mPa.s at 50 °C and from 1.9 to 2.5 mPa.s at 80 °C when the polymer was added to the foaming agent that had SiO_2 NPs. The same qualitative trend for the improvement of the foam apparent viscosity for foam quality of 75% was observed at different temperature conditions, as shown in Figure 12 (a, b, and c).

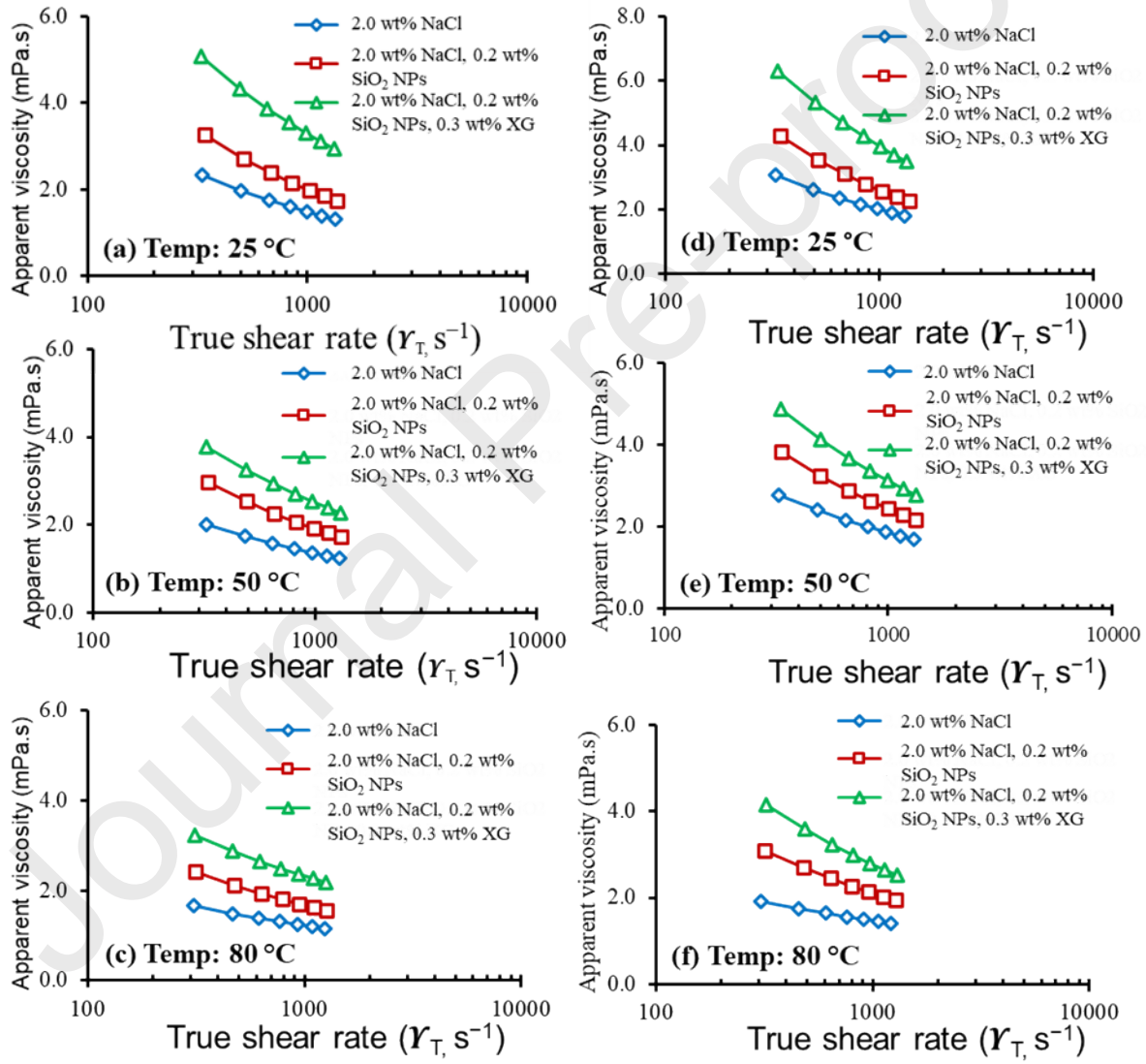

Figure 12. Effect of shear rate on foam apparent viscosity at 0.5 wt% AOS, 2.0 wt% NaCl in the presence of SiO_2 NPs and XG polymer for 75% foam quality (a, b & c), and 95% foam quality (d, e & f) at different temperatures.

Through visual observations we have conducted on the generated bubbles as shown in Figures 13 and 14, the presence of SiO_2 NPs and XG polymer can produce stable and small bubbles

for both foam qualities tested at the three temperatures conditions, compared to the generated bubbles in the absence of SiO_2 NPs and XG polymer. The presence of SiO_2 NPs and XG improved the foam stability leading to a higher pressure drops in the capillary tube flow compared to the foams that are generated in the absence of SiO_2 and XG. Therefore, as the generated bubbles are smaller and uniform, the higher foam apparent viscosity enhancement can be achieved. With increasing the temperature, foam stability decreased, and foam bubbles started to coalesce and become disproportionate; therefore, foam apparent viscosity was decreased.

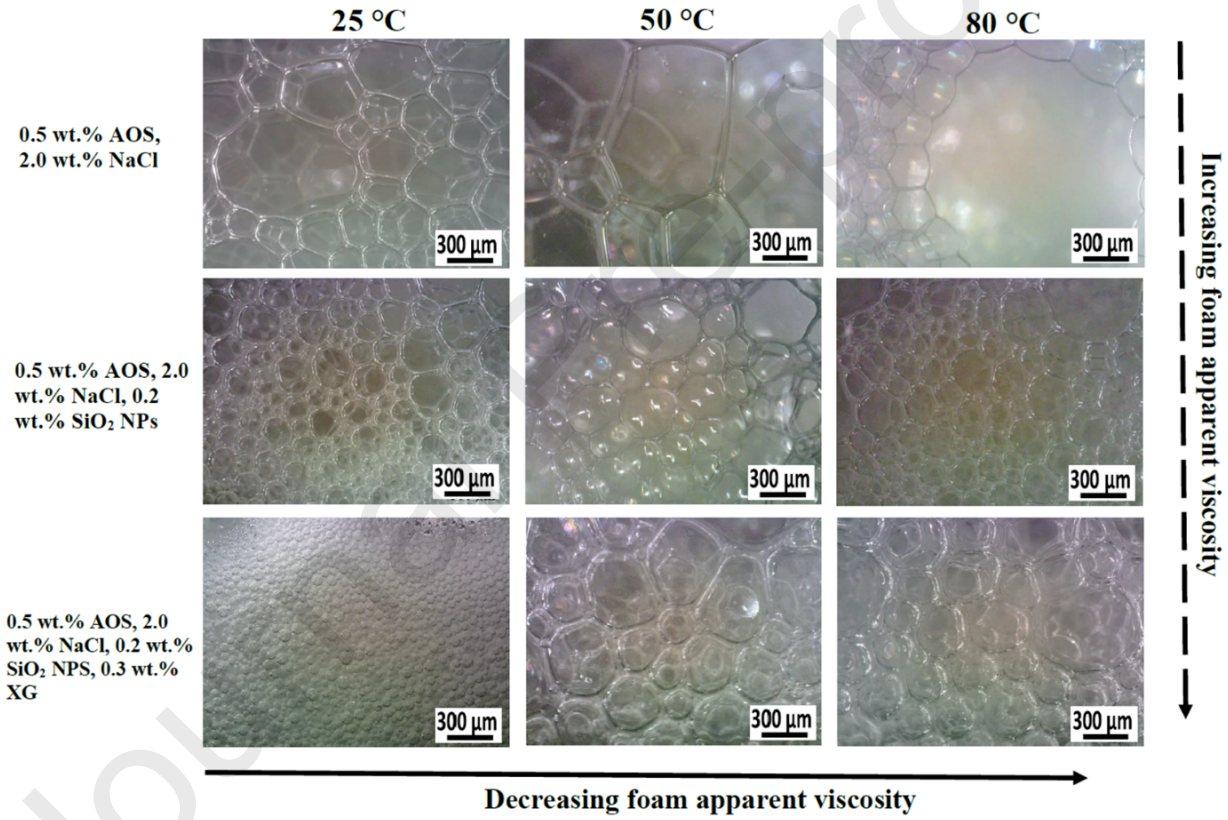

Figure 13. 2D images of foam bubbles generated with the flow rate of 4.2 mL/min (the true shear rates between 300 and 350 s^{-1}) for the foam quality of 75%. The black solid horizontal arrow indicates the decrease of the foam apparent viscosity with elevated temperature conditions, and the black dotted vertical arrow indicates the improvement of the foam apparent viscosity by adding nanoparticles and polymer.

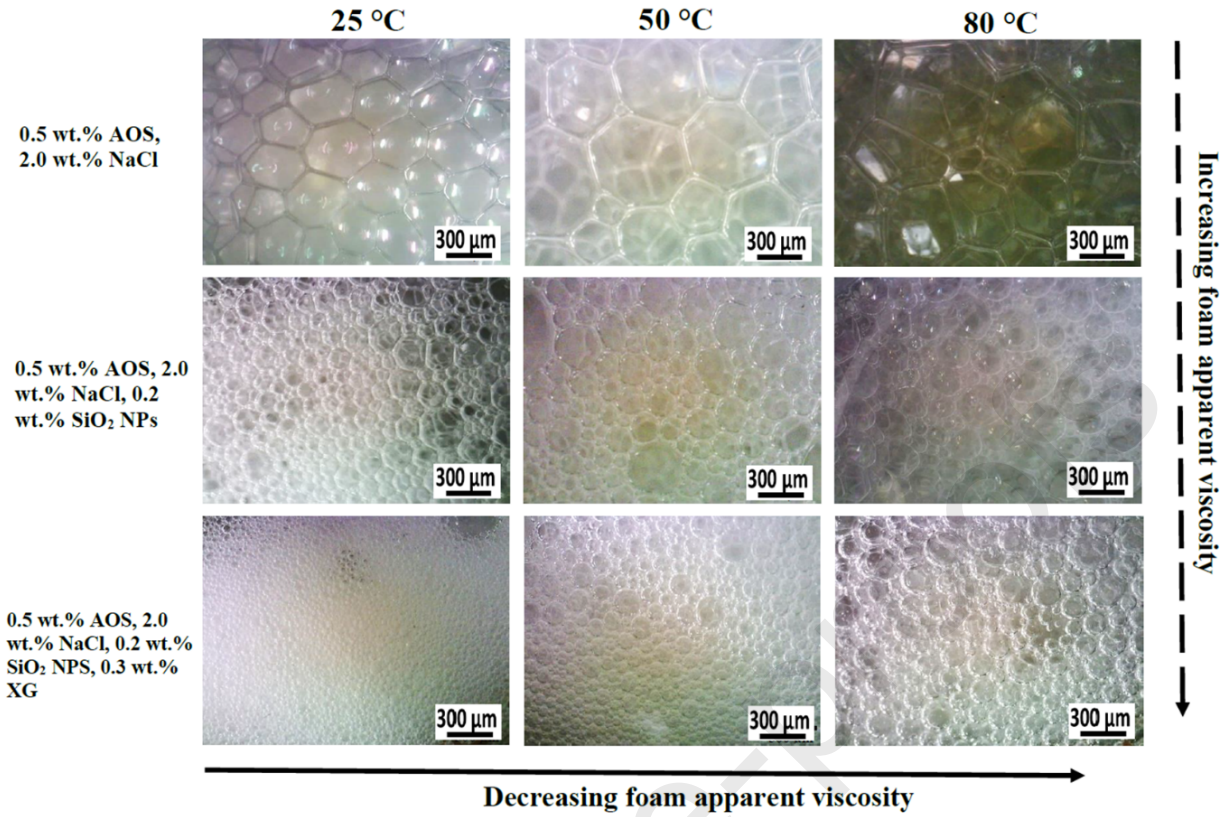

Figure 14. 2D images of foam bubbles generated with the flow rate of 4.2 mL/min (the true shear rates between 300 and 350 s^{-1}) for the foam quality of 95%. The black solid horizontal arrow indicates the decrease of the foam apparent viscosity with elevated temperature conditions, and the black dotted vertical arrow indicates the improvement of the foam apparent viscosity by adding nanoparticles and polymer.

3.5 Foam rheology and power-law model (*n* and *K*)

Based on the results presented in this study, to develop a model that can predict the apparent viscosity of foam; foam quality, composition and temperature should be considered. We used the power law model to capture the impact of these variables on the foam viscosity model. Figure 15 demonstrates the effect of foam quality, temperature, and foam composition on the foam rheological model where the power law index, *n* and consistency index, *K* associated with each foam are presented. The power law index changes slightly as the foam quality and temperature increase, which revealed that *n* is a weak function of the temperature and foam quality. On the other hand, *K* was found to be a strong function of the foam quality and temperature, where the *K* value for any specific colloidal system decreases significantly with increasing the temperature condition, while it increases with increasing the foam quality.

Therefore, the experimental data shown in Figure 15, demonstrates that for each foam composition and quality, the power-law index (n) and the consistency index (K) will change with temperature, and hence their effects should be considered in foam flow modelling.

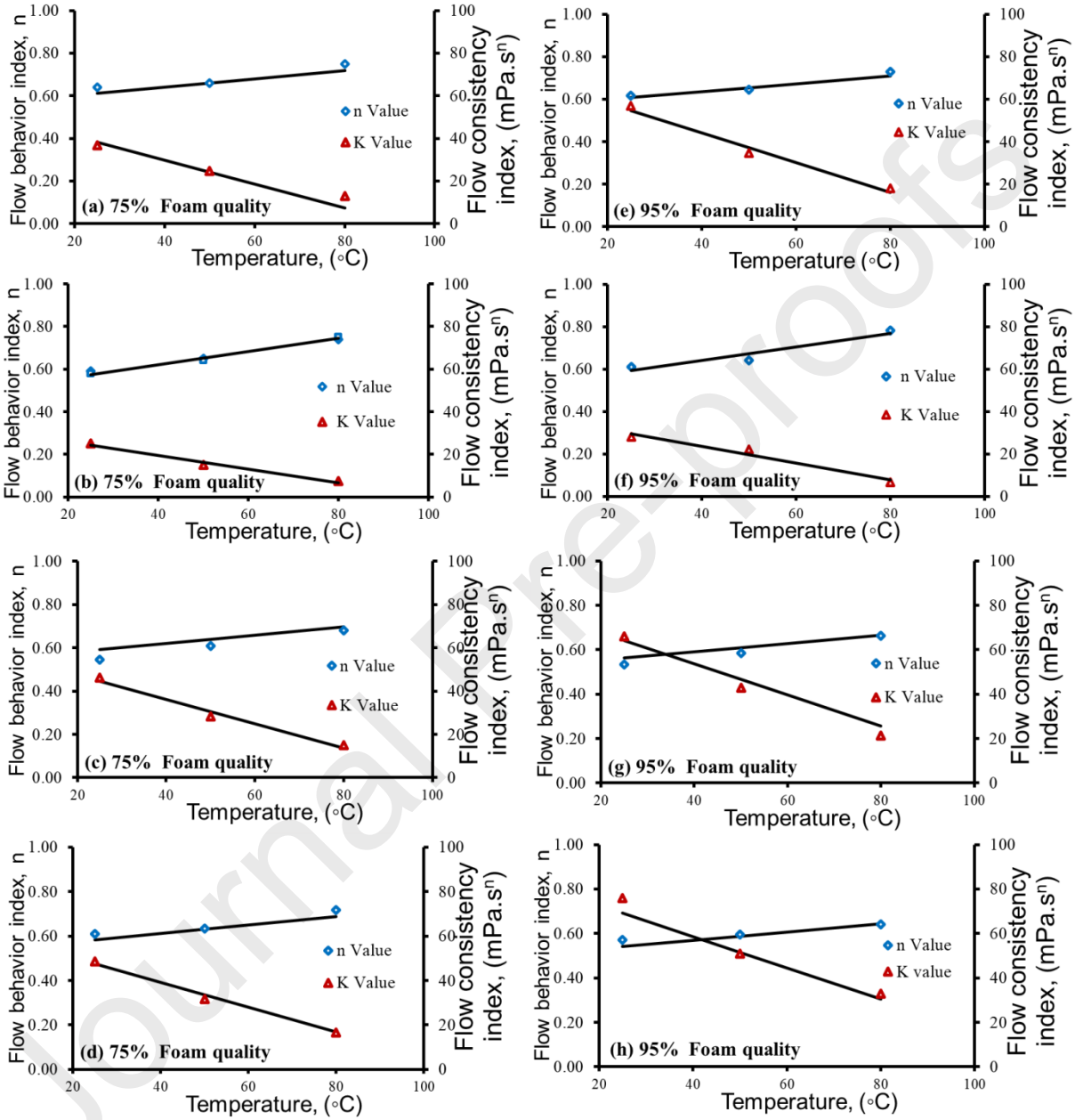

Figure 15. Comparisons of the experimental data for the power-law parameters n and K at different temperatures for CO_2 with 0.5 wt% AOS (a and e), CO_2 with 0.5 wt% AOS & 2.0 wt% NaCl (b and f), CO_2 with 0.5 wt% AOS, 2.0 wt% NaCl & 0.3 wt% SiO_2 (c and g), CO_2 with 0.5 wt% AOS, 2.0 wt% NaCl, 0.2 wt% SiO_2 & 0.3 wt% XG (d and h). The lines of best fit are shown for each set of data.

For any foam composition, the power-law index (n) and the consistency index (K) should be measured at different foam qualities and temperatures, then the 3-D plots associated with K

and *n* can be generated. The surfaces for the power-law index and the consistency index can be inputted to any foam models to allow the estimation of foam apparent viscosity. As an example, Figure 16 shows the 3-D plots for *K* and *n* values as a function of foam quality and temperature which are calculated for the foam generated from AOS solution. Using these 3-D plots, *K* and *n* values will be estimated at any foam quality and temperature and hence foam apparent viscosity for AOS foam is determined. It should be noted that these example surfaces were generated based on 18 experimental data points (six different foam qualities at three temperatures), however, the higher number of data points, the more accurate surfaces. It is also recommended to avoid extrapolation of the surfaces beyond the measured experimental data points.

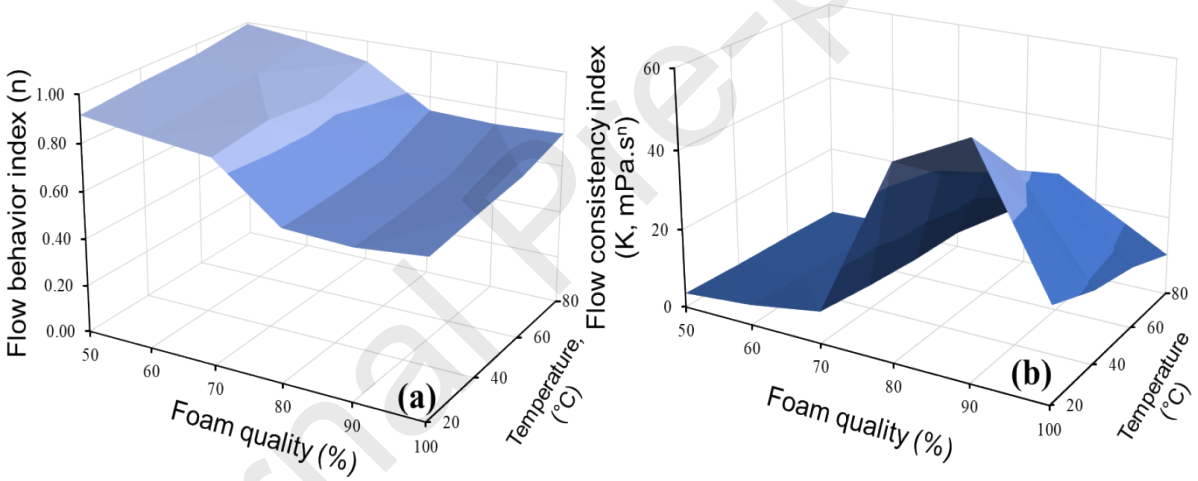

Figure 16. Power-law parameters (a) Flow behavior index, and (b) flow consistency index as a function of foam quality and temperature conditions of AOS foam.

4. Conclusions

In this study, the rheology of the foam with varying temperature conditions was explored. We found that the foam exhibits a shear thinning behaviour and the apparent viscosity strongly depends on the temperature, foam quality, and composition. Higher temperature conditions are detrimental to the foam stability; hence they cause reductions in foam apparent viscosity.

We also found that although at higher salinity conditions foam is less stable, the addition of SiO_2 nanoparticles and xanthan gum polymer increase the foam stability and generate more

uniform and smaller bubbles sizes even at elevated temperature conditions. Generally, foam stability has a direct relation with the foam apparent viscosity, as the foam stability increases, it results in an increase in the foam apparent viscosity. Thus, foam apparent viscosity could be increased in the presence of the optimum concentration of nanoparticles and polymer. This offers an ultimate solution in controlling the foam mobility in narrow channels and porous media where temperature is variable.

In this study we tested the use of the power law model for apparent foam viscosity estimations at different conditions. The results showed that the foam quality, foam composition and temperature are crucial variables that affect the flow behaviour (n) and flow consistency (K) indices of the power law model. Increasing the foam quality (from 75% to 95%) increased the flow consistency index and hence the foam apparent viscosity. On the other hand, increasing the temperature (from 25 to 80 °C) decreased the flow consistency index, and hence the foam apparent viscosity decreased. We also found that the flow behaviour index, is a weak function of temperature and foam quality. Moreover, we used CO_2 as the gas phase to generate the foam in this study, however for any other gases the rheological properties of the foam should be investigated to find accurate values of n and K.

Based on the results of this study, we propose the development of 3-D plots through experimental measurements, and then using them to predict the values of the power-law and the consistency indices at any temperature and foam quality.

5. Acknowledgements

The authors acknowledge the School of Engineering at the University of Aberdeen for providing the required facilities to complete this research; and the financial support from The Carnegie Trust for the Universities of Scotland (RIG70732). Ahmed Bashir would like to thank the Faculty of Engineering University of Khartoum, Sudan for the financial support of his studies at the University of Aberdeen.

6. References

[1] Izgec O, Demiral B, Bertin H J and Akin S 2005 CO_2 Injection in Carbonates SPE West. Reg. Meet. 9.

[2] Dong Z, Li Y, Lin M and Li M 2013 A study of the mechanism of enhancing oil recovery using supercritical carbon dioxide microemulsions Pet. Sci. 10 91-6.

[3] Sharifi Haddad A and Gates I 2017 CO_2-based heavy oil recovery processes for post-CHOPS reservoirs J. CO2 Util. 19 238-46.

[4] Chang S-H and Grigg R B 1999 Effects of Foam Quality and Flow Rate on CO_2-Foam Behavior at Reservoir Temperature and Pressure SPE Reserv. Eval. Eng. 2 248-54.

[5] Pingping S, Xinglong C and Jishun Q 2010 Pressure characteristics in CO_2 flooding experiments Pet. Explor. Dev. 37 211-5.

[6] Chang S-H and Grigg R B 1994 Laboratory Flow Tests Used To Determine Reservoir Simulator Foam Parameters for EVGSAU CO_2 Foam Pilot Permian Basin Oil Gas Recover. Conf. 10.

[7] Jeong S and Corapcioglu M Y 2003 Physical model analysis of foam-TCE displacement in porous media AIChE J. 49 782-8.

[8] Kahrobaei S, Li K, Bonnieu S V and Farajzadeh R 2017 Effects of compositional variations on CO_2 foam under miscible conditions IOR 2017-19th European Symposium on Improved Oil Recovery vol 2017 (European Association of Geoscientists & Engineers) pp 1-12.

[9] Gu M and Mohanty K K 2015 Rheology of polymer-free foam fracturing fluids J. Pet. Sci. Eng. 134 87-96.

[10] Sun X, Liang X, Wang S and Lu Y 2014 Experimental study on the rheology of CO_2 viscoelastic surfactant foam fracturing fluid J. Pet. Sci. Eng. 119 104-11.

[11] Bashir A, Sharifi Haddad A and Rafati R 2018 Experimental Investigation of Nanoparticles/Polymer Enhanced CO_2- Foam in the Presence of Hydrocarbon at High-Temperature Conditions SPE Int. Heavy Oil Conf. Exhib. 13.

[12] Bashir A, Sharifi Haddad A and Rafati R 2019 Nanoparticle/polymer-enhanced alpha olefin sulfonate solution for foam generation in the presence of oil phase at high temperature conditions Colloids Surfaces A Physicochem. Eng. Asp. 582 123875.

[13] Rafati R, Oludara O K, Sharifi Haddad A and Hamidi H 2018 Experimental investigation of emulsified oil dispersion on bulk foam stability Colloids Surfaces A Physicochem. Eng. Asp. 554 110-21.

[14] Gandossi L 2013 An overview of hydraulic fracturing and other formation stimulation technologies for shale gas production.

[15] Ahmed S, Elraies K A, Forooozesh J, Shafian S R B M, Hashmet M R, Hsia I C C and Almansour A 2017 Experimental investigation of immiscible supercritical carbon dioxide foam rheology for improved oil recovery J. Earth Sci. 28 835-41.

[16] Patton J T, Holbrook S T and Hsu W 1983 Rheology of Mobility-Control Foams Soc. Pet. Eng. J. 23 456-60.

[17] Darley H C H and Gray G R 1988 Composition and Properties of Drilling and Completion Fluids (Elsevier Science).

[18] Sanghani V and Ikoku C U 1983 Rheology of foam and its implications in drilling and cleanout operations J. Energy Resour. Technol. 105 362-71.

[19] Firoze Akhtar T, Ahmed R, Elgaddafi R, Shah S and Amani M 2018 Rheological

behavior of aqueous foams at high pressure J. Pet. Sci. Eng. 162 214-24.

[20] Xiao C, Balasubramanian S N and Clapp L W 2017 Rheology of Viscous CO_2 Foams Stabilized by Nanoparticles under High Pressure Ind. Eng. Chem. Res. 56 8340-8.

[21] Li C, Huang Y, Sun X, Gao R, Zeng F B, Tontiwachwuthikul P and Liang Z 2017 Rheological properties study of foam fracturing fluid using CO_2 and surfactant Chem. Eng. Sci. 170 720-30.

[22] Cawiezel K E and Niles T D 1987 Rheological Properties of Foam Fracturing Fluids Under Downhole Conditions SPE Prod. Oper. Symp. 11.

[23] Bonilla L F and Shah S N 2000 Experimental Investigation on the Rheology of Foams SPE/CERI Gas Technol. Symp. 14.

[24] Reidenbach V G, Harris P C, Lee Y N and Lord D L 1986 Rheological Study of Foam Fracturing Fluids Using Nitrogen and Carbon Dioxide SPE Prod. Eng. 1 31-41.

[25] Calvert J R 1990 Pressure drop for foam flow through pipes Int. J. Heat Fluid Flow 11 236-41.

[26] Khan S A, Schnepper C A and Armstrong R C 1988 Foam rheology: III. Measurement of shear flow properties J. Rheol. (N. Y. N. Y). 32 69-92.

[27] Valko P and Economides M J 1992 Volume equalized constitutive equations for foamed polymer solutions J. Rheol. (N. Y. N. Y). 36 1033-55.

[28] Hirasaki G J and Lawson J B 1985 Mechanisms of foam flow in porous media: apparent viscosity in smooth capillaries Soc. Pet. Eng. J. 25 176-90.

[29] Ma K, Mateen K, Ren G, Bourdarot G and Morel D 2018 Modeling foam flow at achievable flow rates in the subterranean formation using the population-balance

approach and implications for experimental design J. Nonnewton. Fluid Mech. 254 36-50.

[30] Lotfollahi M, Farajzadeh R, Delshad M, Varavei A and Rossen W R 2016 Comparison of implicit-texture and population-balance foam models J. Nat. Gas Sci. Eng. 31 184-97.

[31] Rossen W R, Zeilinger S C, Shi J X and Lim M T 1999 Simplified mechanistic simulation of foam processes in porous media SPE J. 4 279-87.

[32] Ozbayoglu M E, Kuru E, Miska S and Takach N 2002 A Comparative Study of Hydraulic Models for Foam Drilling J. Can. Pet. Technol. 41 10.

[33] Deshpande N S and Barigou M 2000 The flow of gas–liquid foams in vertical pipes Chem. Eng. Sci. 55 4297–309.

[34] AlYousif Z, Kokal S, Alabdulwahab A and Gizzatov A 2018 CO_2-Foam Rheology: Effect of Surfactant Concentration, Shear Rate and Injection Quality SPE Kingdom Saudi Arab. Annu. Tech. Symp. Exhib. 12.

[35] Zhang Y, Zhang L, Wang Y, Wang M, Wang Y and Ren S 2015 Dissolution of surfactants in supercritical CO_2 with co-solvents Chem. Eng. Res. Des. 94 624-31.

[36] Chen Y, Elhag A S, Poon B M, Cui L, Ma K, Liao S Y, Reddy P P, Worthen A J, Hirasaki G J, Nguyen Q P, Biswal S L and Johnston K P 2014 Switchable Nonionic to Cationic Ethoxylated Amine Surfactants for CO_2 Enhanced Oil Recovery in High-Temperature, High-Salinity Carbonate Reservoirs SPE J. 19 249-59.

[37] Farhadi H, Riahi S, Ayatollahi S and Ahmadi H 2016 Experimental study of nanoparticle-surfactant-stabilized CO_2 foam: Stability and mobility control Chem. Eng. Res. Des. 111 449-60.

[38] Osei-Bonsu K, Shokri N and Grassia. P 2016 Fundamental investigation of foam flow in a liquid-filled Hele-Shaw cell J. Colloid Interface Sci. 462 288-96.

[39] Khade S D and Shah S N 2004 New Rheological Correlations for Guar Foam Fluids SPE Prod. Facil. 19 77-85.

[40] Sani A M, Shah S N and Baldwin L 2001 Experimental Investigation of Xanthan Foam Rheology SPE Prod. Oper. Symp. 16.

[41] Hunter T N, Wanless E J, Jameson G J and Pugh R J 2009 Non-ionic surfactant interactions with hydrophobic nanoparticles: Impact on foam stability Colloids Surfaces A Physicochem. Eng. Asp. 347 81-9.

[42] Mannhardt K, Schramm L L and Novosad J J 1993 Effect of Rock Type and Brine Composition on Adsorption of Two Foam-Forming Surfactants SPE Adv. Technol. Ser. 1 212-8.

[43] Al-Hashim H S, Celik M S, Oskay M M and Al-Yousef H Y 1988 Adsorption and precipitation behaviour of petroleum sulfonates from Saudi Arabian limestone J. Pet. Sci. Eng. 1 335-44.

[44] Eftekhari A A, Krastev R and Farajzadeh R 2015 Foam Stabilized by Fly-Ash Nanoparticles for Enhancing Oil Recovery.

[45] Worthen A J, Bryant S L, Huh C and Johnston K P 2013 Carbon dioxide-in-water foams stabilized with nanoparticles and surfactant acting in synergy AIChE J. 59 3490-501.

[46] Rafati R, Smith S R, Sharifi Haddad A, Novara R and Hamidi H 2018 Effect of nanoparticles on the modifications of drilling fluids properties: A review of recent advances J. Pet. Sci. Eng. 161 61-76.

[47] Yekeen N, Idris A K, Manan M A, Samin A M, Risal A R and Kun T X 2017 Bulk and

bubble-scale experimental studies of influence of nanoparticles on foam stability Chinese J. Chem. Eng. 25 347-57.

[48] Sarma D S H S R, Pandit J and Khilar K C 1988 Enhancement of stability of aqueous foams by addition of water-soluble polymers-measurements and analysis J. Colloid Interface Sci. 124 339-48.

[49] Verma A, Chauhan G and Ojha K 2017 Synergistic effects of polymer and bentonite clay on rheology and thermal stability of foam fluid developed for hydraulic fracturing Asia-Pacific J. Chem. Eng. 12 872-83.

[50] Ahmed S, Elraies K A, Tan I M and Hashmet M R 2017 Experimental investigation of associative polymer performance for CO_2 foam enhanced oil recovery J. Pet. Sci. Eng. 157 971-9.

[51] Hou Y Y and Kassim H O 2005 Instrument techniques for rheometry Rev. Sci. Instrum. 76 101101.

[52] Prud'homme R K 1995 Foams: Theory: Measurements: Applications (CRC Press, 1995).

[53] Munson B R, Young D F and Okiishi T H 1999 Fundamentals of Fluid Mechanics (John Wiley).

[54] Macosko C W, Larson R G and (Firm) K 1994 Rheology: Principles, Measurements, and Applications (VCH).

[55] Korson L, Drost-Hansen W and Millero F J 1969 Viscosity of water at various temperatures J. Phys. Chem. 73 34-9.

[56] Belhaj A F, Elraies K A, Mahmood S M, Zulkifli N N, Akbari S and Hussien O S 2020 The effect of surfactant concentration, salinity, temperature, and pH on surfactant

adsorption for chemical enhanced oil recovery: a review J. Pet. Explor. Prod. Technol. 10 125-37.

[57] Kapetas L, Vincent Bonnieu S, Danelis S, Rossen W R, Farajzadeh R, Eftekhari A A, Mohd Shafian S R and Kamarul Bahrim R Z 2016 Effect of temperature on foam flow in porous media J. Ind. Eng. Chem. 36 229-37.

[58] Ramadan A, Kuru E and Saasen A 2003 Critcal Review of Drilling Foam Rheology Annu. Trans. Rheol. Soc. 11 63-72.

[59] Chen Y, Elhag A S, Poon B M, Cui L, Ma K, Liao S Y, Omar A, Worthen A, Hirasaki G J and Nguyen Q P 2012 Ethoxylated cationic surfactants for CO_2 EOR in high temperature, high salinity reservoirs SPE Improved Oil Recovery Symposium (Society of Petroleum Engineers).

[60] Weaire D L and Hutzler S 2001 The Physics of Foams (Clarendon Press).

[61] Langevin D 2000 Influence of interfacial rheology on foam and emulsion properties Adv. Colloid Interface Sci. 88 209-22.

[62] Friedmann F and Jensen J A 1986 Some parameters influencing the formation and propagation of foams in porous media SPE California Regional Meeting (Society of Petroleum Engineers).

[63] Jing J, Sun J, Zhang M, Wang C, Xiong X and Hu K 2017 Preparation and rheological properties of a stable aqueous foam system RSC Adv. 7 39258-69.

[64] Rattanaudom P, Shiau B, Suriyapraphadilok U and Charoensaeng A 2019 Aqueous Foam Stabilized by Hydrophobic SiO2 Nanoparticles using Mixed Anionic Surfactant Systems under High-Salinity Brine Condition J. Surfactants Deterg. 22 1247-63.

[65] Jia H, Huang W, Han Y, Wang Q, Wang S, Dai J, Tian Z, Wang D, Yan H and Lv K

2020 Systematic investigation on the interaction between SiO_2 nanoparticles with different surface affinity and various surfactants J. Mol. Liq. 304 112777.

[66] Shojaei M J, Méheust Y, Osman A, Grassia P and Shokri N 2021 Combined effects of nanoparticles and surfactants upon foam stability Chem. Eng. Sci. 238 116601.

Highlights:

- Foam viscosity is a function of composition, temperature, and foam quality
- Foam viscosity can be modelled using a power law model
- n and K (power law model) change at different temperatures and foam qualities
- 3-D plots of viscosity parameters can be generated from the laboratory tests

Ahmed Bashir: Investigation, Methodology, Validation, Visualization, Writing - Original Draft. **Amin Sharifi Haddad:** Conceptualization, Methodology, Funding acquisition, Supervision, Formal analysis, Project administration, Writing - Review & Editing. **Roozbeh Rafati**: Supervision, Methodology, Writing - Review & Editing.

Declaration of interests

☒ The authors declare that they have no known competing financial interests or personal relationships that could have appeared to influence the work reported in this paper.

☐The authors declare the following financial interests/personal relationships which may be considered as potential competing interests: